

RESEARCH

Open Access



# Respiratory pathogen dynamics in community fever cases: Jiangsu Province, China (2023–2024)

Fei Deng<sup>1†</sup>, Zhuhan Dong<sup>2†</sup>, Tian Qiu<sup>3</sup>, Ke Xu<sup>1</sup>, Qigang Dai<sup>1</sup>, Huiyan Yu<sup>1</sup>, Huan Fan<sup>1</sup>, Haifeng Qian<sup>3</sup>, Changjun Bao<sup>1</sup>, Wei Gao<sup>3</sup> and Liguozhu<sup>2,4,5\*</sup>

## Abstract

**Background** Respiratory infectious diseases have the highest incidence among infectious diseases worldwide. Currently, global monitoring of respiratory pathogens primarily focuses on influenza and coronaviruses. This study included influenza and other common respiratory pathogens to establish a local respiratory pathogen spectrum. We investigated and analyzed the co-infection patterns of these pathogens and explored the impact of lifting non-pharmaceutical interventions (NPIs) on the transmission of influenza and other respiratory pathogens. Additionally, we used a predictive model for infectious diseases, utilizing the commonly used An autoregressive comprehensive moving average model (ARIMA), which can effectively forecast disease incidence.

**Methods** From June 2023 to February 2024, we collected influenza-like illness (ILI) cases weekly from the community in Xuanwu District, Nanjing, and obtained 2046 samples. We established a spectrum of respiratory pathogens in Nanjing and analysed the age distribution and clinical symptom distribution of various pathogens. We compared age, gender, symptom counts, and viral loads between individuals with co-infections and those with single infections. An autoregressive comprehensive moving average model (ARIMA) was constructed to predict the incidence of respiratory infectious diseases.

**Results** Among 2046 samples, the total detection rate of respiratory pathogen nucleic acids was 53.37% (1092/2046), with influenza A virus 479 cases (23.41%), influenza B virus 224 cases (10.95%), and HCoV 95 cases (4.64%) being predominant. Some pathogens were statistically significant in age and number of symptoms. The positive rate of mixed infections was 6.11% (125/2046). There was no significant difference in age or number of symptoms between co-infection and simple infection. After multiple iterative analyses, an ARIMA model (0,1,4), (0,0,0) was established as the optimal model, with an  $R^2$  value of 0.930, indicating good predictive performance.

**Conclusions** The spectrum of respiratory pathogens in Nanjing, Jiangsu Province, was complex in the past. The primary age groups of different viruses were different, causing various symptoms, and the co-infection of viruses did not correlate with the age and gender of patients. The ARIMA model estimated future incidence, which plateaued in subsequent months.

**Keywords** Acute respiratory tract infection, Pathogen spectrum, ARIMA model, Virus, Bacteria

<sup>†</sup>Fei Deng and Zhuhan Dong contributed equally to this article. Author order was determined by drawing straws.

\*Correspondence:

Liguozhu

zhuliguozhu2002@163.com; njxwcdc@163.com

Full list of author information is available at the end of the article



## Introduction

Global Burden of Disease (GBD) studies show that respiratory infectious diseases cause approximately 145,000 deaths globally every year [1]; in 2019, the number of cases of upper respiratory tract infection was as high as 17.2 billion, accounting for 42.83% of all disease cases in the GBD database. The incidence rate was the highest [2], posing a massive threat to global human health. Currently, respiratory tract infections rank second in the worldwide burden of disease among children and adolescents, making it one of the leading causes of rising morbidity and mortality worldwide [3]. The susceptible population of respiratory infectious diseases is broad, and the transmission route is easy to achieve, often caused by a variety of pathogens. The infection situation is complex and frequently overlapping, so detection is usually tedious [4]. Currently, there is more research in China on monitoring and controlling novel coronaviruses and influenza viruses [5, 6], with less focus on monitoring other pathogens. This study conducts multi-pathogen testing on feverish populations in Xuanwu District, Nanjing City, establishes a local respiratory pathogen spectrum, understands the epidemiological patterns of pathogens, and provides more basis for diagnosing and treating respiratory infections in patients with unknown pathogens in clinical practice.

From 2019 to 2023, the world experienced a pandemic of the novel coronavirus (COVID-19). As the virulence of COVID-19 weakened, community transmission decreased, and vaccination coverage became more widespread, the severity of COVID-19 appeared to decline. However, it still poses a threat due to its strong infectivity [7]. In recent years, China and other countries have explored the impact of non-pharmaceutical interventions (NPIs) [8–10] related to novel coronavirus on the prevalence of respiratory infectious diseases. NPIs refer to measures to delay the spread of epidemics in addition to vaccination and taking drugs, which aim to reduce the spread of infectious diseases by minimizing the exposure rate of the general population [11–13]. These measures include wearing masks, washing hands frequently, opening windows for ventilation, social distancing, closing schools, businesses and other social places, and canceling large public gatherings. The application of these measures has dramatically reduced the morbidity of Acute respiratory infectious disease. However, most studies did not include the period after NPIS were gradually lifted. We analyzed the alterations in the prevalence trends of influenza and other respiratory pathogens after the removal of NPIs, aiming to assess the potential ramifications of easing such restrictions on other respiratory infectious diseases. Collecting the current spectrum of respiratory pathogens can prevent and control the present and future

respiratory infectious diseases, and help provide more reference opinions for public health decision-making.

In epidemiology, modeling technology is commonly used for early prediction and warning of infectious diseases [14, 15]. Box and Jenkins proposed the Autoregressive Integrated Moving Average (ARIMA) model in 1976 [16]. The ARIMA model is a time series forecasting method that analyses time series to make short-term predictions. It has been used to predict hand, foot, and mouth disease, COVID-19, Hepatitis B, etc. In previous studies, some scholars found that the ARIMA model was superior to other models.

In conclusion, in this study, we chose the ARIMA model to predict the number of future infectious diseases in Nanjing. Establishing effective and accurate predictive models to forecast the future trends of respiratory tract infections in the Xuanwu District of Nanjing City can play a role in early warning and monitoring. This can provide data support for formulating response strategies and implementing prevention and control measures, transitioning from passive to active prevention.

## Methods

### Study design and participant enrollment

The study was conducted in Xuanwu District, Nanjing City, from June 2023 to February 2024, jointly carried out by the Jiangsu Provincial Center for Disease Control and Prevention (Jiangsu CDC) and the Xuanwu District Center for Disease Control and Prevention in Nanjing City. A weekly collection of influenza-like cases with respiratory infections such as fever (temperature  $\geq 37$  °C) accompanied by cough or sore throat was done from the community. The study was approved by the Institutional Review Board of Jiangsu CDC (No. JSJK2022-B016-02). All participants have provided written informed consent for demographic characteristics, physical examinations, medical records, and sample tests.

### Pathogen detection

Throat swab specimens during the acute phase were collected from patients (not less than 40 samples per week) by professional personnel following standard operating procedures. The specimens were immediately placed in sterilized sampling tubes containing 3 ml of sampling fluid and transported to the Jiangsu Provincial Center for Disease Control and Prevention laboratory within 48 h under 4 °C conditions for testing.

**Nucleic Acid Extraction:** Nucleic acids were extracted using the Rapid Viral Nucleic Acid Extraction Kit (manufactured by Tianlong Science and Technology Co., Ltd., Xi'an, China), with the extraction process carried out using the Tianlong GeneRotex 96 Automatic Nucleic Acid Extractor, following the manufacturer's instructions.

**Nucleic Acid Detection:** The nucleic acids of respiratory pathogens were detected using the 16 Respiratory Pathogens Nucleic Acid Detection Kit (produced by Biotech Co., Ltd., Beijing, China) through real-time quantitative PCR. PCR amplification was performed according to the kit instructions, and results were determined accordingly.

These respiratory pathogens mainly included influenza A (Flu A), influenza B (Flu B), respiratory syncytial virus (RSV), Herpes simplex virus (HSV), human adenovirus (HADV), Enteroviruses (EV), human coronavirus (HCoV), Parainfluenza virus (HPIV), Human rhinovirus (HRV), human Bocavirus (HBoV), Human metapneumovirus (HMPV), *Streptococcus pneumoniae* (*S. pneumoniae*), *Haemophilus influenzae* (*H. influenzae*), *Mycoplasma pneumoniae* (*M. pneumoniae*), *Chlamydia pneumoniae* (*C. pneumoniae*).

This study conducted a pathogen composition analysis of various respiratory pathogens, identifying the predominant pathogen genotypes to provide a basis for further control of respiratory infectious diseases. For EV and HRV typing, the respiratory multi-pathogen detection kit (Shuo Shi, JC20302) is used for initial RNA screening from the specimens. Positive samples for enterovirus detection undergo serotyping using the enterovirus 71 type, coxsackievirus (CV) A16 type RNA detection kit (Shuo Shi, JC20302), and CV A6 type, A10 type RNA detection kit (Shuo Shi, JC20205). Non-EV71/CVA16/CVA6/CVA10 specimens undergo sequencing typing, with amplification primer sequences as follows: OL68-1:5'-GGTAAATTCCACCACCANCC-3' and EVP2:5'-CCTCCGGCCCCCTGAATGCGGCTAAT-3'. PCR reaction conditions are set at 50 °C for reverse transcription for 30 min, 95 °C for denaturation for 15 min, followed by 35 cycles of 95 °C for 30 s, 52 °C for 45 s, 72 °C for 90 s, and a final extension at 72 °C for 5 min. The amplified products are validated using QIAxcel capillary electrophoresis before being sent to Shanghai Sangon Biotechnology Co., Ltd. for sequencing.

Results were double-entered by two experimenters using Epidata, including sample number, nucleic acid test result (positive/negative), viral load, date of testing, and clinical symptoms to ensure data accuracy. Data were analyzed using GraphPad Prism 9.5.0 and SPSS version 27.0 software (IBM, New York, USA).

#### ARIMA model

The ARIMA model, as one of the standard methods in time series analysis, reflects the development trend of time series data from the perspective of autocorrelation. It combines three components, autoregressive (AR), differencing (I), and moving average (MA), to capture trends and seasonal information in time series data. The order of the autoregressive and moving average parts

is 'p' and 'q,' represented by AR (p) and MA (q) respectively, and 'd' is the number of differences (order) made to make them a stationary series. This study constructed an ARIMA model based on weekly incidence data from June 2023 to February 2024. The Augmented Dickey-Fuller (ADF) test was performed using Eviews 12.0 and SPSS 27.0 for processing.

Methods of ARIMA model construction [17–19]:

- (1) **Data Pre-processing:** The data were checked for missing values and imputed where necessary. The weekly number of respiratory pathogen incidents was then imported as raw data to create a time series.
- (2) **Stationarity of the Series:** Before applying the ARIMA model, assessing the stationarity of the time series is crucial. Stationarity was initially evaluated using a scatterplot, the autocorrelation function (ACF), and the partial autocorrelation function (PACF). The ADF test was conducted using Eviews 12.0 software to confirm stationarity. The series appeared to stabilize after first-order differencing, while seasonal differencing led to instability, confirming stationarity in conjunction with the ADF unit root test.
- (3) **Determine ARIMA Model Parameters:** The parameters of the ARIMA model were determined by observing the PACF to identify the p-value (the order of the autoregressive term), the ACF to identify the q-value (the order of the moving average term), and the differencing order to determine the d-value (the number of differencing required).
- (4) **Construct the ARIMA Model:** The appropriate time series model was constructed based on the identified characteristics. ACF and PACF plots were generated, and first-order differencing indicated zero-lag autocorrelation and partial autocorrelation. The best-fitting model was selected using the Akaike Information Criterion (AIC) and the Bayesian Information Criterion (BIC). By testing different combinations of p, d, and q values, the model with the lowest AIC and BIC was chosen.
- (5) **Model Validation:** After selecting the final model, the Ljung-Box test was used to check whether the residual sequence constituted white noise. The residuals should be statistically insignificant in the residual correlation test, confirming that they are white noise. If residual autocorrelation is detected, the model should be re-evaluated and adjusted until white noise is confirmed.
- (6) **Prediction Using the Validated Model:** The validated model was then used for prediction. Model fit was evaluated by checking whether the actual

values fell within the 95% confidence interval of the predicted values or by assessing the mean absolute percentage error (MAPE).

**Table 1** Demographic and Clinical Characteristics of Positive Cases

| Variable                  | N (%)             |
|---------------------------|-------------------|
| Mean Age ± SD             | 36.8 ± 20.6 years |
| <i>Age group</i>          |                   |
| < 14                      | 148(13.55)        |
| 14–59                     | 733(67.12)        |
| > 59                      | 211(19.32)        |
| <i>Gender</i>             |                   |
| Male                      | 467(42.77)        |
| Female                    | 625(57.23)        |
| <i>Pathogen detection</i> |                   |
| Simple infection          | 967(88.55)        |
| Mixed infection           | 125(11.45)        |
| <i>Clinical Symptoms</i>  |                   |
| Cough                     | 874(79.60)        |
| Headache                  | 479(43.62)        |
| Sore throat               | 640(58.29)        |
| Muscle pain               | 346(31.51)        |
| Nasal congestion          | 388(35.34)        |
| Runny nose                | 504(45.90)        |
| Fatigue                   | 516(46.99)        |

## Results

### Demographic results

Samples were collected weekly from June 2023 to February 2024, totaling 2046 samples. Among them, 1092 samples tested positive, resulting in an overall positive rate of 53.37%. The mean age was 36.8 ± 20.6 years, with the highest number of individuals in the 14–59 age group (733, 67.12%). There were 467 males (42.77%) and relatively more females (625, 57.23%). Among them, 125 individuals tested positive for mixed infections, accounting for 11.45%, while 968 individuals had single infections, accounting for 88.48%. The most common symptoms were cough 874 cases (79.60%), Sore throat 640 cases (58.29%), and Fatigue 516 cases (46.99%) (Table 1).

### Respiratory virus infection rate

The most common pathogen was Flu A, with a positive rate of 23.41% (479 cases) (Fig. 1), all of which were H3N2 subtypes. This was followed by Flu B at 10.95% (224 cases), all typed as B.Victoria. HCoV accounted for 4.64% (95 cases), including 33 cases of HCoV-229E, 50 cases of HCoV-OC43, 11 cases of HCoV-HKU1, and 1 case of HCoV-NL63. HRV accounted for 4.06% (83 cases), sequencing of rhinovirus with simple infection, including 18 cases of Rhinovirus A, 3 cases of Rhinovirus B, and 17 cases of Rhinovirus C. HMPV accounted for 3.81% (78 cases). HPIV accounted for 3.2% (65 cases), RSV for 2.25% (46 cases) (including 14 cases of RSV A ON1 and 32 cases of RSV B BA9), HADV for 2.0% (41 cases), HSV for 1.2% (29 cases), EV for 0.24% (5 cases) (including 1 case of CVA21, 3 cases of CVA6, and 1 case of D68). *M.*

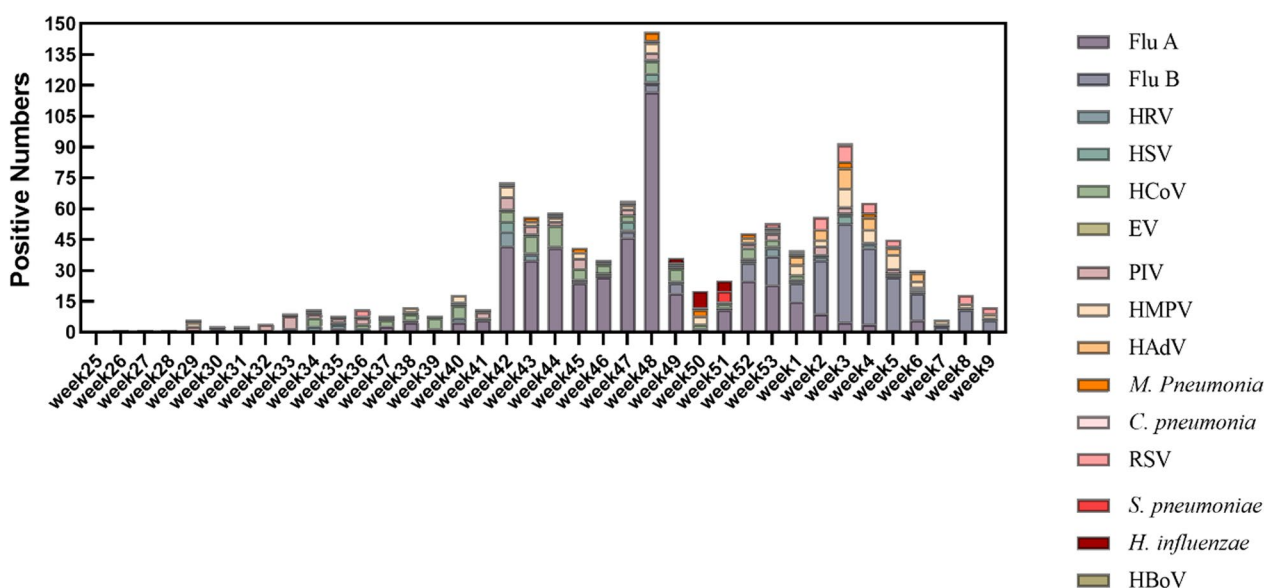


**Fig. 1** Weekly positive detection rate of respiratory pathogens from week 25, 2023 to week 9, 2024

*Pneumonia* accounted for 1.08% (22 cases), *H. influenzae* for 0.7% (15 cases), *S. pneumoniae* for 0.34% (7 cases), HBoV for 0.1% (2 cases), and *C. pneumoniae* for 0.1% (2 cases). *M. Pneumonia*, and HADV infections are more common in children under 14 years old. In contrast, Flu A, Flu B, HCoV, and HRV infections mainly occur in the 14–59 age group, with elderly individuals being more susceptible to HMPV infections (Table 2).

Except for RSV, all other pathogens can cause symptoms such as cough, headache, sore throat, muscle pain, nasal congestion, runny nose, and fatigue. Among these, *H. influenzae* (43, 21.83%), HMPV (59, 24.08%), HADV (38, 30.16%), Flu A (380, 22.77%), HPIV (23, 23.96%), and HCoV (165, 24.59%) infections commonly present with cough as the predominant symptom. HPIV (20, 20.83%) is the pathogen most likely to cause sore throat, while runny nose is most commonly associated with HADV infection (21, 16.67%). Please refer to Table 3 for details.

The positive rate for mixed infections was 6.11% (125 out of 2046), with double infection accounting for 5.82% (119/2046), triple infection for 0.24% (5/2046), and quadruple infection for 0.05% (1/2046). The detection rate of Flu A + HRV is the highest in mixed infections at 20.69% (24 cases) followed by FluA + HCoV at 8.62%, (10 cases) and FluA + HSV at 11.11% (9 cases) (Fig. 2). Flu A was mostly co-infected with other pathogens. Simultaneous or sequential infection of respiratory pathogens may lead to mixed infections, causing antagonistic or synergistic effects among pathogens and altering the severity of the disease. Comparative analysis was conducted between mixed infections and single infections based on Ct values,

gender, age, and number of symptoms. (Table 4). In the cases of single infection, there were 585 females (58.15%) and 421 males (41.85%). There were 49 males (41.17%) for double-mixed infections and 70 females (58.82%). In cases of multiple mixed infections, there were 2 males (33.33%) and 4 females (66.67%). The differences were not statistically significant ( $p > 0.05$ ). In different age groups, there was no statistical significance between simple infection and co-infection in the age group, and age did not affect co-infection. The pathogens in both simple and mixed infections most commonly caused cases to exhibit two symptoms, with 235 cases (24.38%) for simple infection and 34 cases (27.20%) for mixed infection. However, there was no statistically significant difference in the number of symptoms caused by the infection ( $p > 0.05$ ). the ct value of simple infection HSV was larger, and the difference in Ct value was statistically significant (Table 5).

The study data was compared with respiratory pathogen surveillance data from Beijing [5] and Jinan [20] during the NPIs. The total positive detection rate in Beijing was 10.97% during the NPIs period. The top five pathogen positives, from highest to lowest, were HCoV (2.42%), HRV (2.17%), HPIV (1.71%), Flu A and Flu B (1.50%), and RSV (1.23%). In Jinan, the overall positive detection rate was 40.18%. Among the top five pathogens, the positive rates were 9.85% for HRV, 8.94% for *M. Pneumonia*, 6.53% for RSV, 3.13% for HPIV, and 2.16% for HADV.

In this study, the positive detection rate began to increase in week 38 of 2023 (September 11–17) and peaked in week 41 (October 2–8), with the highest

**Table 2** Positive detection rates of respiratory pathogens in different age groups

| Pathogens            | < 14 years (n,%) | 14–59 years (n,%) | > 59 years (n,%) | $\chi^2$ | P value |
|----------------------|------------------|-------------------|------------------|----------|---------|
| HBoV                 | 0(0.00)          | 2(0.25)           | 0(0.00)          | 0.584*   | –       |
| HSV                  | 2(1.20)          | 20(2.50)          | 7(3.00)          | 1.232*   | 0.559   |
| <i>S. pneumoniae</i> | 0(0.00)          | 5(0.60)           | 2(0.90)          | 0.954*   | 0.620   |
| <i>C. pneumoniae</i> | 0(0.00)          | 2(0.25)           | 0(0.00)          | 0.584*   | –       |
| <i>M. Pneumonia</i>  | 12(7.30)         | 10(1.30)          | 0(0.00)          | 23.693*  | <0.001  |
| <i>H. influenzae</i> | 3(1.80)          | 9(1.10)           | 3(1.30)          | 0.901*   | 0.625   |
| HMPV                 | 8(4.90)          | 33(4.20)          | 32(15.90)        | 41.322   | <0.001  |
| HADV                 | 25(15.20)        | 13(1.60)          | 3(1.30)          | 79.755   | <0.001  |
| Flu A                | 48(29.30)        | 344(43.30)        | 87(37.30)        | 12.169   | 0.002   |
| Flu B                | 43(18.50)        | 159(20.00)        | 22(9.40)         | 13.892   | <0.001  |
| EV                   | 0(0.00)          | 5(0.60)           | 0(0.00)          | 1.197*   | 0.510   |
| HPIV                 | 7(4.30)          | 43(5.40)          | 13(5.60)         | 0.406    | 0.808   |
| HCoV                 | 4(2.40)          | 60(7.60)          | 31(13.30)        | 16.053   | <0.001  |
| HRV                  | 8(4.90)          | 55(6.90)          | 20(8.60)         | 2.045    | 0.369   |
| RSV                  | 4(2.40)          | 34(4.30)          | 8(3.40)          | 1.387    | 0.504   |

P < 0.05 shows that the difference is significant.

\*Denotes Fisher exact probability method.

**Table 3** Clinical symptom distribution of participants infection with respiratory pathogens

| Pathogens            | Cough      | Headache   | Sore throat | Muscle pain | Nasal congestion | Runny nose | Fatigue    | $\chi^2$ | P value |
|----------------------|------------|------------|-------------|-------------|------------------|------------|------------|----------|---------|
| HRV                  | 49(20.16)  | 30(12.35)  | 47(19.34)   | 25(10.29)   | 27(11.11)        | 37(15.23)  | 28(11.52)  | 19.54    | 0.003   |
| EV                   | 3(15.00)   | 3(15.00)   | 2(10.00)    | 3(15.00)    | 3(15.00)         | 2(10.00)   | 4(20.00)   | 1.419*   | 0.996   |
| HSV                  | 19(19.39)  | 14(14.29)  | 13(13.27)   | 10(10.20%)  | 14(14.29)        | 15(15.31)  | 13(15.00)  | 3.667    | 0.738   |
| <i>S. pneumoniae</i> | 5(25.00)   | 3(15.00)   | 3(15.00)    | 2(10.00)    | 1(5.00)          | 3(15.00)   | 3(15.00)   | 3.596*   | 0.768   |
| <i>M. Pneumonia</i>  | 20(26.67)  | 11(14.67)  | 10(13.33)   | 7(9.33)     | 9(12.00)         | 10(13.33)  | 8(10.67)   | 12.133   | 0.060   |
| HPIV                 | 43(21.83)  | 22(11.17)  | 33(16.75)   | 19(9.64)    | 24(12.18)        | 30(15.23)  | 26(13.20)  | 16.203   | 0.013   |
| HCoV                 | 59(24.08)  | 34(13.88)  | 48(19.59)   | 25(10.20)   | 22(8.98)         | 27(11.02)  | 30(12.24)  | 38.8     | <0.001  |
| RSV                  | 38(30.16)  | 12(9.52)   | 23(18.25)   | 4(3.17)     | 17(13.49)        | 21(16.67)  | 11(8.73)   | 46.407   | <0.001  |
| Flu A                | 380(22.77) | 214(12.82) | 280(16.78)  | 153(9.17)   | 163(9.77)        | 225(13.48) | 254(15.22) | 175.066  | <0.001  |
| <i>H. influenzae</i> | 12(19.35)  | 8(12.90)   | 12(19.35)   | 7(11.29)    | 6(9.68)          | 7(11.29)   | 10(16.13)  | 4.855    | 0.582   |
| HMPV                 | 55(26.57)  | 23(11.11)  | 36(17.39)   | 18(8.70)    | 22(10.63)        | 31(14.98)  | 22(10.63)  | 38.731   | <0.001  |
| HADV                 | 23(23.96)  | 15(15.63)  | 20(20.83)   | 11(11.46)   | 7(7.29)          | 8(8.33)    | 12(12.50)  | 18.326   | 0.005   |
| Flu B                | 165(24.59) | 87(12.97)  | 112(16.69)  | 60(8.94)    | 70(10.43)        | 85(12.67)  | 92(13.71)  | 87.714   | <0.001  |
| HBoV                 | 1(10.00)   | 2(20.00)   | 1(10.00)    | 1(10.00)    | 2(20.00)         | 2(20.00)   | 1(10.00)   | 1.856*   | –       |
| <i>C. pneumoniae</i> | 2(25.00)   | 1(12.50)   | 0(0.00)     | 1(12.50)    | 1(12.50)         | 1(12.50)   | 2(12.50)   | 3.227    | 0.964   |

P < 0.05 shows that the difference is significant.

\*Denotes Fisher exact probability method.

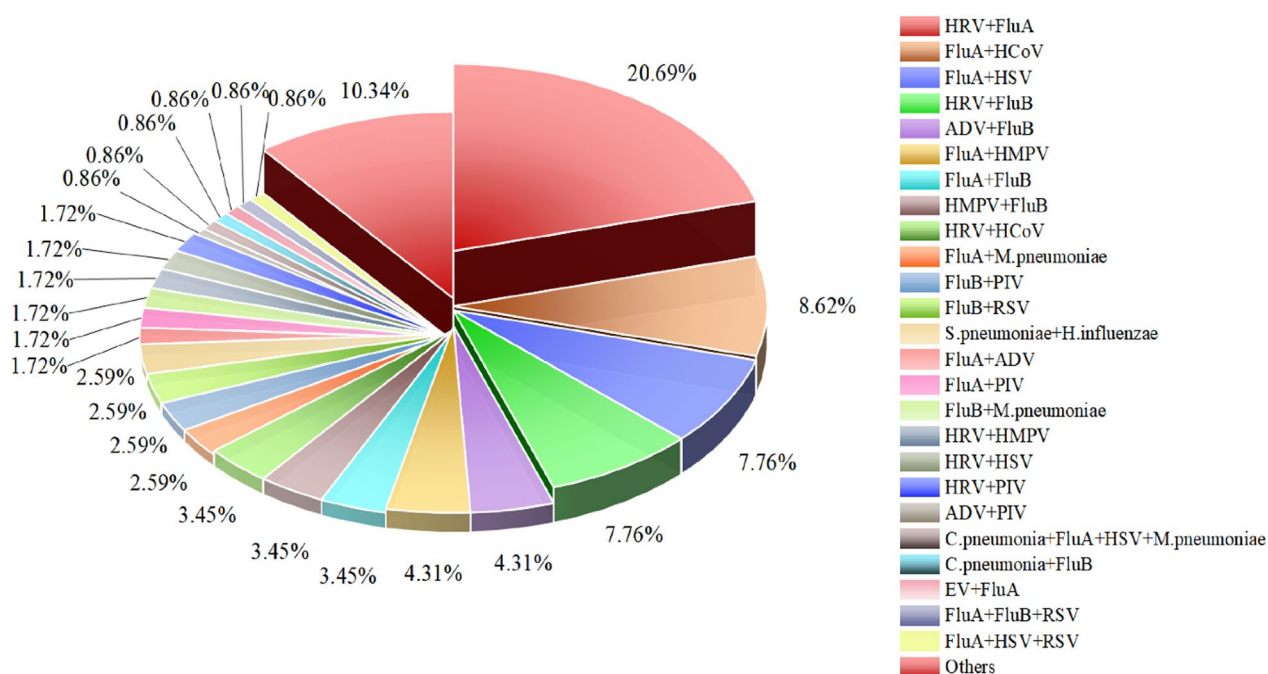


**Fig. 2** Proportion of multi-pathogen mixed infection status

number of positive cases recorded in week 48 (November 20–26) (Fig. 3A). Influenza maintained a high level throughout the monitoring period. Flu A detection peaked in week 48 (November 20–26) with a positive rate of 62.6% and remained high from week 41, 2023, to week 1, 2024 (October 2–January 7). Flu B showed a high rate from week 52, 2023, to week 6, 2024 (December

18, 2023–February 11, 2024). HRV and HCoV detection peaked in week 39 (September 18–24) and gradually declined (Fig. 3B). EV, HPIV, HMPV, and RSV were detected throughout the monitoring period but with relatively low detection rates. HADV had a relatively higher detection rate from week 52, 2023, to week 6, 2024, while *H. influenzae* and *S. pneumoniae* were detected in

**Table 4** Characteristics of simple and mixed infections in positive cases

|                           | Simple infection (N,%) | Co-infection (N,%) |           | $\chi^2$ | P value |
|---------------------------|------------------------|--------------------|-----------|----------|---------|
|                           |                        | 2                  | > 2       |          |         |
| <i>Gender</i>             |                        |                    |           |          |         |
| Male                      | 417(43.12)             | 49(41.17)          | 2(33.33)  | 0.388    | 0.821*  |
| Female                    | 550(56.88)             | 70(58.82)          | 4(66.67)  |          |         |
| <i>Age group(yr)</i>      |                        |                    |           |          |         |
| < 14                      | 125(12.03)             | 23(19.33)          | 0(0.00)   | 6.000    | 0.158*  |
| 14–59                     | 656(65.20)             | 71(59.66)          | 6(100.00) |          |         |
| > 59                      | 186(18.49)             | 25(21.01)          | 0(0.00)   |          |         |
| <i>Number of symptoms</i> |                        |                    |           |          |         |
| 1                         | 216(22.50)             | 22(18.49)          | 1(16.67)  | 10.189   | 0.496*  |
| 2                         | 235(24.48)             | 33(27.73)          | 1(16.67)  |          |         |
| 3                         | 156(16.25)             | 20(16.81)          | 2(33.33)  |          |         |
| 4                         | 110(11.46)             | 14(11.76)          | 0(0.00)   |          |         |
| 5                         | 102(10.62)             | 8(6.72)            | 0(0.00)   |          |         |
| 6                         | 61(6.35)               | 9(7.56)            | 2(33.33)  |          |         |
| 7                         | 80(8.33)               | 13(10.92)          | 0(0.00)   |          |         |

P < 0.05 shows that the difference is significant.

\* Denotes fisher exact probability method.

**Table 5** Comparison of Ct Values between Simple Infection and Co-Infection

| Pathogens            | Simple infection (N,%) | Mixed infection(N,%) | t     | P value |
|----------------------|------------------------|----------------------|-------|---------|
| HRV                  | 29.67                  | 28.93                | 0.919 | 0.057   |
| EV                   | 31.10                  | 32.16                | 0.568 | 0.806   |
| HSV                  | 34.57                  | 32.55                | 1.661 | 0.042   |
| <i>S. pneumoniae</i> | 34.47                  | 32.55                | 0.605 | 0.936   |
| <i>M. Pneumonia</i>  | 33.34                  | 27.62                | 4.577 | 0.666   |
| HPIV                 | 27.19                  | 27.43                | 2.344 | 0.723   |
| HCoV                 | 29.38                  | 29.65                | 0.206 | 0.685   |
| RSV                  | 31.16                  | 31.58                | 0.25  | 0.086   |
| Flu A                | 27.19                  | 27.43                | 0.345 | 0.423   |
| <i>H. influenzae</i> | 32.14                  | 32.94                | 0.107 | 0.213   |
| HMPV                 | 27.79                  | 29.21                | 1.047 | 0.727   |
| HADV                 | 31.13                  | 32.84                | 1.060 | 0.824   |
| Flu B                | 27.15                  | 27.17                | 0.019 | 0.213   |

P < 0.05 shows that the difference is significant.

weeks 49–51 (November 27–December 17) and were not detected during other times.

**Building the ARIMA model**

**Stabilizing the series**

A model was established based on weekly incidence data from June 2023 to February 2024, and a time series plot

was generated. The time series plot showed non-stationarity. Next, the stationarity of the series was confirmed using the Augmented Dickey–Fuller (ADF) unit root test in Eviews software, after conducting trend and intercept tests, with a reported  $t = -3.37$ ,  $p\text{-value} > 0.05$ . Thus, the original time series required stabilization. A transformed time series plot was generated after applying a first-order difference ( $d = 1$ ). It was visually assessed for stationarity and tapering, indicating improved stationarity. The ADF unit root test yielded a  $p\text{-value} < 0.01$ , confirming basic stationarity. However, seasonal differencing increased instability, so a first-order difference was chosen [Supplementary Fig. 1].

**Model identification**

ACF and PACF plots were generated for the transformed series, showing zero-lag autocorrelation and partial autocorrelation after first-order differencing. ARIMA (0,1,4) (0,0,0) was selected as the optimal model after testing different  $p$ ,  $d$ , and  $q$  values. The model had an  $R^2$  value of 0.930, and the standardized Bayesian Information Criterion (BIC) value was the smallest among all fitted models at 5.338. A residual test using Ljung-Box  $Q = 10.930$  and  $p = 0.691$  confirmed that the residual sequence was white noise. The mean absolute percentage error (MAPE) and predicted values was 34.181, indicating a good model fit [Supplementary Fig. 2].

**Model fitting**

Based on the weekly number of cases from June 2023 to February 2024, the ARIMA (0,1,4) (0,0,0) model was constructed. The optimal model was used to predict the number of respiratory pathogens until June 2024, as shown in the graph (Fig. 4). The actual number of cases, as seen from the table, all fall within the 95% confidence interval of the predicted values, indicating a good fit of the model (Table 6).

**Discussion**

Large and medium-sized cities have a concentrated population, apparent seasonal climate, and high incidence of respiratory infectious diseases. This study focused on monitoring multiple respiratory pathogens in feverish populations in Nanjing communities to establish a respiratory pathogen spectrum and fill the gap in acute respiratory infectious disease monitoring after the cessation of NPIs. The study showed that from week 42 (October 2023), there was a rapid increase in positive pathogen samples, maintaining a stable and high positive detection rate, dropping in December and then showing a growth trend until early February 2024. This study conducted molecular epidemiological research on respiratory pathogens to identify dominant genotypes. This contributes

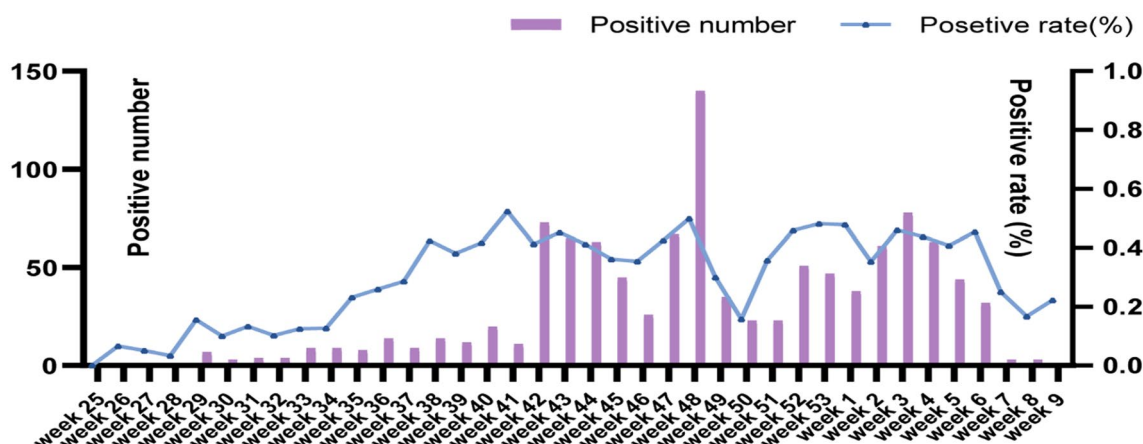


**Fig. 3** Number of positive cases and positive detection rate of respiratory pathogens per week

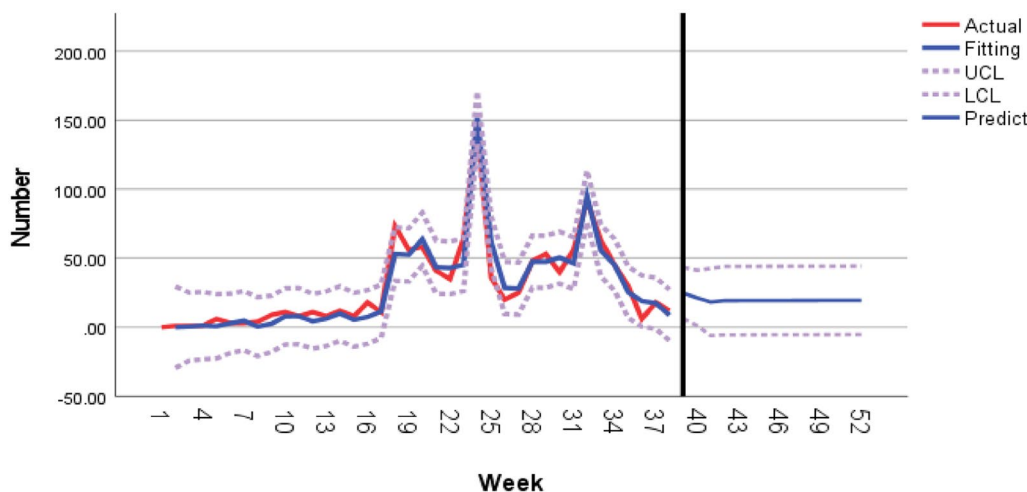


**Fig. 4** The ARIMA model fitting

**Table 6** Actual and predicted number of positive cases of respiratory pathogens

| Date                        | Actual | Fitting | 95%CI         |
|-----------------------------|--------|---------|---------------|
| 20–26 November 2023         | 146    | 151.98  | 132.99–170.96 |
| 27 November–3 December 2023 | 36     | 61.86   | 43.00–80.72   |
| 4–10 December 2023          | 20     | 28.59   | 9.73–47.44    |
| 11–17 December 2023         | 25     | 28.08   | 9.23–46.93    |
| 18–24 December 2023         | 48     | 47.52   | 28.76–66.29   |
| 25–31 December 2023         | 53     | 47.4    | 28.65–66.15   |
| 1–7 January 2024            | 40     | 50.38   | 31.63–69.12   |
| 8–14 January 2024           | 56     | 46.36   | 27.67–65.05   |
| 15–21 January 2024          | 92     | 94.94   | 76.28–113.6   |
| 22–28 January 2024          | 63     | 55.59   | 36.93–74.24   |
| 29 January–4 February 2024  | 45     | 45.12   | 26.48–63.75   |

to a deeper understanding of the epidemiological characteristics of different pathogens, including their transmission routes, infectivity, and seasonal distribution. This study’s overall positive detection rate was 53.57%, with high detection rates for Flu A and Flu B (24.00% and 10.95%, respectively). All Flu A subtypes were H3N2, while all Flu B subtypes were B/Victoria lineage. Influenza viruses showed a peak in winter and spring, with Flu A prevalent from October to January and Flu B prevalent from December to February, consistent with research in Beijing [21]. However, our study’s high detection rate of influenza viruses indicates a severe influenza situation in our city.

HRV was prevalent from August to October, consistent with research in Taizhou [22]. This study conducted

typing tests on simple infection of rhinoviruses and enteroviruses, detecting a total of 18 strains of rhinovirus A, including 3 of type A21, 2 of type A64, 2 of type A7, 1 of type A71, and 3 of type A98, as well as 3 strains of rhinovirus B, including 1 of type B69, and 17 strains of rhinovirus C, including 2 of type C1. It can be observed that the detection rates of HRV A and C types are relatively high, consistent with domestic and international research results [23, 24]. HRV-A and HRV-C are more likely to cause moderate to severe diseases, and type C is associated with childhood asthma attacks. Therefore, strengthening the monitoring of rhinovirus typing is of great significance for preventing and controlling respiratory infectious diseases. In enteroviruses, 3 strains of CV A6, 1 strain of CV A21, and 1 strain of enterovirus D68 were detected. CV A6 has become one of the main pathogens causing human hand-foot-and-mouth disease in recent years. While CV A21 and enterovirus D68 can also enter the body through the respiratory tract, they rarely cause hand-foot-and-mouth disease and herpangina, mainly manifesting as symptoms of upper respiratory tract infections. HPIV, HCoV, HSV, EV, and HADV showed short-term low prevalence. Among them, HPIV is mainly type HPIV-3, and among the four serotypes, the infection rate of HPIV-3 is the highest, often peaking in the winter and spring seasons, consistent with previous research findings [25]. HCoV mainly invaded the upper respiratory tract with HCoV-OC43 and HCoV-229E types. HMPV, *H. influenzae*, *S. pneumoniae*, and *C. pneumoniae* had relatively low annual detection rates, appearing sporadically. However, due to the short duration of our study and the lack of coverage in the spring, it is not sufficient to fully describe the common respiratory pathogen prevalence characteristics in the region, requiring further supplementation in the future.

Mixed infections of pathogens may pose challenges to the diagnosis, treatment, and epidemic prevention and control of respiratory infections. Concurrent or sequential infection of respiratory pathogens may lead to mixed infections, causing positive synergistic or negative antagonistic interactions among pathogens, leading to varying degrees of disease severity changes in patients. Pathogen interactions can be categorized into three modes: (1) viral interference, (2) viral synergy, and (3) no interaction. Viral interference, also known as antagonism, occurs when the infection by the first virus reduces the replication of the second virus within the host. In contrast, viral synergy, or enhancement, refers to a situation where the first virus may enhance the infection of the second virus [26]. In this study, mixed infections accounted for 11.45% of total positive cases, with Flu A mostly co-infected with other pathogens, and the highest positive detection rates in mixed infections were observed for Flu A + HRV,

FluA + HCoV, FluA + HSV. Previous studies suggested negative interactions between IAV and RSV, HRV and IAV, while RSV and HRV co-infections indicated increased disease severity [26]. Previous studies have shown that [27], co-infections may lead to an increased hospitalization rate among patients with respiratory viral infections, indicating an escalation in disease severity. This study conducted a comparative analysis of single infections and co-infections based on gender, different age groups, Ct values, and the number of symptoms. The results ultimately revealed statistically significant differences between single infections and co-infections across different age groups. The lack of statistical significance in symptom numbers may be due to the challenge of deriving conclusions about severity solely based on symptom counts. HRV, HSV, *M. Pneumoniae*, and *S. pneumoniae* in mixed infections had smaller Ct values than single infections, possibly due to synergistic effects between pathogens, resulting in increased disease severity. The Ct value for HSV single infection was 34.57, while for mixed infection, it was 32.55, with significant differences and higher persuasiveness. However, HADV and HMPV single infection had larger Ct values, possibly related to their role as primary infecting viruses activating the host's non-specific innate immune response. Due to the short study period and relatively low number of mixed infection cases, significant results could not be obtained. Viral interference may provide a new model for antiviral treatment research. Some studies have shown that Influenza A virus Defective Interfering Particles (IAV-DIPs) can stimulate the host's innate immune system to inhibit HSV infection and replication [28], suggesting a potential preventive and therapeutic role in respiratory infectious diseases. Some studies [29, 30] have also shown that the antagonistic effects between viruses were closely related to the reduction in the severity of diseases caused by respiratory viral infections. For example, HRV infection was found to decrease the probability of infection with influenza A (H1N1 subtype). There is limited research in China in this area, and future monitoring of more data can lead to further research. Subsequent follow-up tracking or research based on hospital cases could further investigate this matter. Currently, there is limited research on viral interference in China. Further studies on the types of viral interactions and the mechanisms underlying viral interference can provide valuable insights for the formulation of public health policies, the development of vaccines, and the strategies for controlling acute respiratory infections.

Starting in January 2023, China lifted control measures for COVID-19 from Class A infectious diseases. This study was conducted from June 2023 to the end of February 2024 after a comprehensive relaxation of epidemic

control measures. The aim was to explore the changes in the respiratory pathogen spectrum after the cessation of NPIs. Since the emergence of COVID-19, China has implemented NPIs, including encouraging mask-wearing, patient isolation, social distancing, hand hygiene, and disinfection to prevent new SARS-CoV-2 infections. Comparing the spectrum of respiratory pathogens in Jinan City and Beijing City during NPIs period with that in this study, the overall positive detection rate of pathogens in this study (54.15%) was significantly higher than that in Jinan City (40.18%) and Beijing (10.97%), indicating that NPIs measures against COVID-19 significantly reduced the prevalence of respiratory pathogens.

Furthermore, the detection rate of influenza in this study was 34.95% (24.00% + 0.95%), which was significantly higher than 3.44% in Jinan City and 1.5% in Beijing City, and the positive detection rate of all pathogens in this study was higher than that in Beijing city, possibly because NPIs measures during COVID-19 not only prevented the invasion of viruses but also cut off the transmission of other respiratory pathogens. However, the overall positive rate of respiratory pathogens is rising, which may be linked to the public's relaxation of vigilance against respiratory infectious diseases. It may also be related to the immune debt after the novel coronavirus pandemic, resulting in a rebound or high epidemic level of some infectious diseases. However, during NPIs, the positive rate of HRV pathogens in Jinan City was 9.85%, higher than 8.7% in this study, which may be since HRV is transmitted through direct or indirect contact with contaminated items, which requires chlorine-based disinfectants to eradicate, and the use of ethanol is less effective. In addition, the positive rates of *Mycobacterium pneumoniae* and respiratory syncytial virus in Jinan were significantly higher than in our study, which may be because our study focussed on community populations rather than hospital-based studies, and that Jinan has a higher proportion of children under the age of 15, who are more susceptible to these pathogens.

In recent years, there has been extensive research in China utilizing the ARIMA model for infectious disease surveillance and prediction, demonstrating its effectiveness, particularly in short-term forecasting [31, 32]. Based on the scientifically predicted results of the model, early detection of respiratory pathogen trends can be achieved, providing timely warnings for control efforts and facilitating the targeted formulation of prevention and control strategies. In this study, fitting models were established using the ARIMA model (0,1,4), (0,0,0) based on influenza surveillance data from June 2023 to February 2024. According to the forecast results of the ARIMA model, influenza peaks are expected to occur in late autumn and winter of 2023, with the number of

detected respiratory pathogens projected to decline initially from March to June 2024 before stabilizing. This trend may be attributed to the rising temperatures during the spring and summer seasons. Nanjing, characterized by a subtropical monsoon climate, experiences a noticeable temperature increase by the end of February, along with high humidity and rainfall. Studies have indicated that the transmission of respiratory viruses is associated with climate conditions, especially humidity and temperature, with respiratory pathogens being more likely to spread under cold and dry conditions [33]. Additionally, this study has certain limitations as it only considers the quantity of detected pathogens, potentially leading to underreporting or overreporting biases in weekly data.

Overall, our study monitored respiratory infections in the community population of Nanjing City, providing insights into the spectrum and co-infections of respiratory pathogens. A time series forecasting model has been established to serve as a reference for prevention and control efforts. While filling gaps in Nanjing's respiratory pathogen spectrum research, our study has limitations due to a short period and single sample source. Future research could involve hospital samples to understand respiratory pathogens' epidemiology further, establish a more comprehensive pathogen spectrum, and enhance Nanjing's monitoring and alert system post-COVID-19 pandemic.

### Supplementary Information

The online version contains supplementary material available at <https://doi.org/10.1186/s12985-024-02494-9>.

Additional file 1.

### Author contributions

Fei Deng was responsible for completing most of the experimental work and contributed to the data collation. Zhuhan Dong did all the data collection and analysis, and she wrote the first draft of the manuscript. Fei Deng and Zhuhan Dong contributed equally to this article. Author order was determined by drawing straws. Tian Qiu, Ke Xu, Qigang Dai, Huiyan Yu, Huan Fan, Haifeng Qian, and Changjun Bao participated in the analysis and interpretation of all data. Liguozhu designed the project, planned the experiments, verified the data collection, analysis and interpretation, and revised the original manuscript into the final version submitted. All authors reviewed the manuscript, agreed to take responsibility for all aspects of the work, and testified to the accuracy and completeness of the work.

### Funding

This work was supported by National Key R&D Program of China (2023YFC2605100, 2023YFC2605102).

### Availability of data and materials

No datasets were generated or analysed during the current study.

### Declarations

#### Ethics approval and consent to participate

Our study did not require further ethics committee approval as it did not involve animal or human clinical trials and was not unethical. By the ethical

principles outlined in the Declaration of Helsinki, all participants provided informed consent before participating in the study. The anonymity and confidentiality of the participants were guaranteed, and participation was completely voluntary.

#### Consent for publication

All authors approved the final manuscript and the submission to this journal.

#### Competing interests

The authors declare no competing interests.

#### Author details

<sup>1</sup>Department of Acute Infectious Disease Control and Prevention, Jiangsu Provincial Center for Disease Control and Prevention, Nanjing, China. <sup>2</sup>Nanjing Medical University, Nanjing, China. <sup>3</sup>Xuanwu District Center for Disease Control and Prevention, Nanjing, China. <sup>4</sup>NHC Key Laboratory of Enteric Pathogenic Microbiology, Jiangsu Provincial Center for Disease Control and Prevention, Nanjing, China. <sup>5</sup>Jiangsu Provincial Medical Key Laboratory of Pathogenic Microbiology in Emerging Major Infectious Diseases, Jiangsu Provincial Center for Disease Control and Prevention, Nanjing, China.

Received: 27 June 2024 Accepted: 8 September 2024

Published online: 20 September 2024

#### References

- GBD 2017 Influenza Collaborators. Mortality, morbidity, and hospitalizations due to influenza lower respiratory tract infections, 2017: an analysis for the Global Burden of Disease Study 2017. *Lancet Respir Med*. 2019;7(1):69–89.
- Yang J, McClymont H, Wang L, Vardoulakis S, Hu W. Epidemic features of COVID-19 and potential impact of hospital strain during the omicron wave—Australia, 2022. *China CDC Wkly*. 2023;5(7):165–9.
- Jin X, Ren J, Li R, et al. Global burden of upper respiratory infections in 204 countries and territories, from 1990 to 2019. *EclinicalMedicine*. 2021;37:100986.
- Zhou L, HAN Z-Z, Zhang X-L, Xu R-R, Chen YF, Chen X. Detection and analysis of 22 respiratory pathogens in Yangzhou area. *Chin J Health Lab Tec*. 2023; 33(18): 2191–2194.
- Zhang J, Yang T, Zou M, Wang L, Sai L. The epidemiological features of respiratory tract infection using the multiplex panels detection during COVID-19 pandemic in Shandong province, China. *Sci Rep*. 2023;13(1):6319.
- Zhao P, Cul G, Wu X. Pathogenic spectrum analysis of adult cases of respiratory tract infection in Beijing, 2017–2020. *South China J Prevent Med*. 2022;37(05):45–7.
- Ye C, Zhang G, Zhang A, et al. The omicron variant reinfection risk among individuals with a previous SARS-CoV-2 infection within one year in Shanghai, China: a cross-sectional study. *Vaccines*. 2023;11(7):1146.
- Liu P, Xu M, Cao L, et al. Impact of COVID-19 pandemic on the prevalence of respiratory viruses in children with lower respiratory tract infections in China. *Viol J*. 2021;18(1):159.
- Shi HJ, Kim NY, Eom SA, et al. Effects of non-pharmacological interventions on respiratory viruses other than SARS-CoV-2: analysis of laboratory surveillance and literature review from 2018 to 2021. *J Korean Med Sci*. 2022;37(21): e172.
- Yan H, Zhai B, Yang F, Wang P, Zhou Y. The impact of non-pharmacological interventions measures against COVID-19 on respiratory virus in preschool children in Henan. *China J Epidemiol Glob Health*. 2024;14(1):54–62.
- ÓhAiseadha C, Quinn GA, Connolly R, et al. Unintended consequences of COVID-19 non-pharmaceutical interventions (NPIs) for population health and health inequalities. *Int J Environ Res Public Health*. 2023;20(7):5223.
- Bedford J, Enria D, Giesecke J, et al. COVID-19: towards controlling of a pandemic. *Lancet*. 2020;395(10229):1015–8.
- Ye Q, Liu H. Impact of non-pharmaceutical interventions during the COVID-19 pandemic on common childhood respiratory viruses—an epidemiological study based on hospital data. *Microbes Infect*. 2022;24(1): 104911.
- Hu X-S, Shao Y, Zhang W-L, Chen K, Gao Y. Characteristic analysis and prediction of hospital influenza-like illness based on ARIMA mode. *Hosp Manag Forum*. 2023;40(12):10–3.
- Claris S, Peter N. Arima model in predicting of Covid-19 epidemic for the southern Africa region. *Afr J Infect Dis*. 2022;17(1):1–9.
- Box GEP. Time series analysis, forecasting and control rev. San Francisco: Holden-Day; 1976.
- Ilie OD, Ciobica A, Doroftei B. Testing the accuracy of the ARIMA models in forecasting the spreading of COVID-19 and the associated mortality rate. *Medicina*. 2020;56(11):566.
- Qi B, Liu N, Yu S, Tan F. Comparing COVID-19 case prediction between ARIMA model and compartment model—China, December 2019–April 2020. *China CDC Wkly*. 2022;4(52):1185–8.
- Wang L, Liang C, Wu W, et al. Epidemic situation of brucellosis in Jinzhou city of China and prediction using the ARIMA model. *Can J Infect Dis Med Microbiol*. 2019;2019:1429462.
- Dong M, Luo M, Li A, et al. Changes in the pathogenic spectrum of acute respiratory tract infections during the COVID-19 epidemic in Beijing, China: a large-scale active surveillance study. *J Infect*. 2021;83(5):607–35.
- Lin Z, Xiang G, Chong Z, et al. Epidemiological characteristics of respiratory pathogen infection in patients with respiratory tract infection in Tongzhou district, Beijing from 2020 to 2022. *Disease Surveillance*. 2021;47(03):296–300.
- Ding W, Zha J. Pathogen monitoring results of people with acute respiratory infection in Taizhou, 2016–2017. *Mod Prevent Med*. 2019;46(13):2436–9.
- Xie JM, Huang XX. Prevalence and molecular typing of rhinoviruses in people with severe acute infection of the respiratory tract in Guangdong province, China, 2019–2021. *Chin J Virol*. 2023;39(2):364–71.
- Li Wanwei Yu, Bo ZJ, et al. Genetic diversity and epidemiology of human rhinovirus among children with severe acute respiratory tract infection in Guangzhou, China. *Viol J*. 2021;18(1):174.
- Parsons J, Korsman S, Smuts H, et al. Human parainfluenza virus (HPIV) detection in hospitalized children with acute respiratory tract infection in the western cape, South Africa during 2014–2022 reveals a shift in dominance of HPIV 3 and 4 infections. *Diagnostics*. 2023;13(15):2576.
- Piret J, Boivin G. Viral interference between respiratory viruses. *Emerg Infect Dis*. 2022;28(2):273–81.
- Asner SA, Science ME, Tran D, Smieja M, Merglen A, Mertz D. Clinical disease severity of respiratory viral co-infection versus single viral infection: a systematic review and meta-analysis. *PLoS ONE*. 2014;9(6): e99392.
- Pelz L, Piagnani E, Marsall P, et al. Broad-spectrum antiviral activity of influenza a defective interfering particles against respiratory syncytial, yellow fever, and zika virus replication in vitro. *Viruses*. 2023;15(9):1872.
- Casalegno JS, Ottmann M, Duchamp MB, et al. Rhinoviruses delayed the circulation of the pandemic influenza A (H1N1) 2009 virus in France. *Clin Microbiol Infect*. 2010;16(4):326–9.
- Gilbert-Girard S, Piret J, Carbonneau J, Hénaut M, Goyette N, Boivin G. Viral interference between severe acute respiratory syndrome coronavirus 2 and influenza A viruses. *PLoS Pathog*. 2024;20(7):e1012017.
- Tang L, Lv W, Bao L, et al. Predictive analysis of influenza-like cases in Chifeng based on ARIMA model predictive analysis. *Chin J Soc Med*. 2023;40(03):350–4.
- Xiaojiang Z, Han Z, Qiyin W, Mengliang Ye. Prediction of influenza in Chongqing, China, based on the autoregressive integrated moving average model. *J Chongqing Med Univ*. 2023;48(12):1425–9.
- Sloan C, Moore ML, Hartert T. Impact of pollution, climate, and sociodemographic factors on spatiotemporal dynamics of seasonal respiratory viruses. *Clin Transl Sci*. 2011;4(1):48–54.

#### Publisher's Note

Springer Nature remains neutral with regard to jurisdictional claims in published maps and institutional affiliations.